EXPERIMENTAL STUDY ON ELECTRICAL CONDUCTIVITY AND DIELECTRIC STUDIES OF TRIPOTASSIUM SODIUM DICHROMATE SINGLE CRYSTAL

Kavita[1], Dr. Praveen Kumar[2]

Department of Chemistry

[1,2]OPJS University, Churu (Rajasthan) – India

Abstract

The $K_3Na(CrO_4)_2$ or KNCr crystal has a place with a group of compounds, with the regular chemical formula $A_3C(BX_4)_2$ (where A, C = Li, Na, K, Rb, Cs, NH_4; BX_4 = SO_4, SeO_4, CrO_4), which as often as possible show ferroic phases. Experimental investigations of these materials demonstrate that K_3Na $(SO4)_2$, K_3Na $(CrO_4)_2$ and K_3Na $(SeO_4)_2$ experience ferroelastic phase transitions from a point group $\bar{3}$ m1 to 2/m at around 70 K, 239 K and at 346 K, separately. Notwithstanding the consistent second – arrange phase transition at 239 K, KNCr shows another structural phase transition at 853 K with symmetry diminishment likely from 6/mmm to $\bar{3}$ m. The ferroelastic phase transition of KNCr is joined by movements of two crystallographically independent K+ cations, and additionally by move and tilting of $[CrO_4]^{2-}$. Mroz et al. Performed Brillouin scattering examines and proposed a Landau model to give a subjective portrayal of the ferroelastic transition. Electron paramagnetic reverberation thinks about recommends the presence of an incommensurate phase. From acoustic investigations, inconsistencies were found close to the ferroelectric phase transition.

1. INTRODUCTION

Madariaga et al. have considered the crystal structure of KNCr and detailed that the crystal at room temperature phase is trigonal with space group P $\bar{3}$ m1, and it has cell dimensions, a = 5.858 (6) Å and c = 7.523 (2) Å. The density of the crystal is 2.77(2) g cm-3. The structure is developed of CrO4 tetrahedra, NaO6 octahedra and two extraordinary, K (1) O_{10} and K (2) O_{12}, more convoluted polyhedra stacked along the c-axis. The melting point of the crystal is 1160 K . The Na-O separates in the NaO6 octahedra are symmetry limited to a single value of 2.364 Å. The mean separations in the K (1) O_{10} and K (2) O_{12} polyhedra are 2.969 Å and 3.155 Å individually. The Cr-O separations range from

1.613 Å to 1.6459 Å. The values of the two conceivable bond angles O-Cr-O, in the CrO4 group (110.31° and 108.63°),

Show a little bending concerning the perfect tetrahedral con Figureuration. The structural investigation of the room-temperature phase (P$\bar{3}$m1) announced that the structure is isomorphous to K3Na (SO4)2 . The structures of the high and low-temperature phases of the undifferentiated from compound $K_3Na(SeO_4)_2$ have been comprehended by Fabry et al. which uncovered that the high temperature phase of K_3Na $(SeO_4)_2$ is isomorphous to the room-temperature phases of K_3Na $(SO_4)_2$ and K_3Na $(CrO_4)_2$.
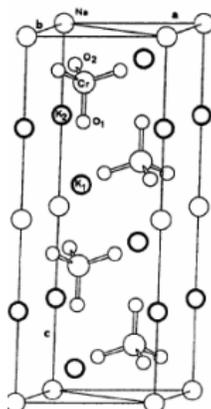
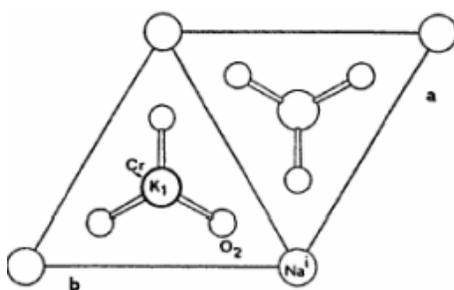**Figure 1: Trigonal phase of $K_3Na(CrO_4)_2$ crystal.**

Figure 2: View along the c - axis of $K_3Na(CrO_4)_2$ crystal.

Figure 1 demonstrates the room temperature phase (trigonal) of K_3Na $(CrO_4)_2$ single crystal with two unit cells which are connected by the cross section interpretation along the c-axis. Figure 2 is a perspective of the trigonal phase of K_3Na $(CrO4)_2$ single crystal along the c-axis.

A genuinely total audit of the past examinations on KNCr single crystal is itemized. This section incorporates the aftereffects of the electrical conductivity and dielectric contemplates did in KNCr single crystal. These measurements in KNCr crystal are accounted for out of the blue.

2. EXPERIMENTAL TECHNIQUE
Sample Preparation

Single crystals of KNCr were grown at constant temperature of 315 K from saturated watery solutions by moderate evaporation strategy. The stock reagents utilized for the blend were chemically unadulterated sodium and potassium hydroxides and chromic corrosive anhydride. The result of union was sanitized by three-overlap recrystallization from distilled water. Marginally yellow very much shaped crystals were gotten with a most extreme edge length of around 20 mm over a time of 40-45 days. The temperature of the shower is kept up at a constant temperature of 315 K and controlled to an accuracy of $\pm$ 0.05 K utilizing the digitally programmable temperature controller. The points of interest of the apparatus utilized for the crystal growth have been discussed in part 2. Amid the growth, the crystal was consistently pivoted in both clockwise and against clockwise directions utilizing the crystal rotation system. The photograph of the grown crystal is appeared in Figure3. An illustration of the morphology of the crystal is appeared in Figure4.
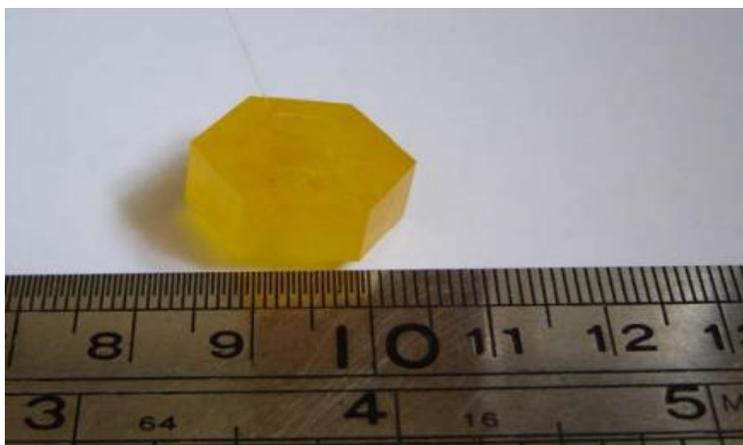
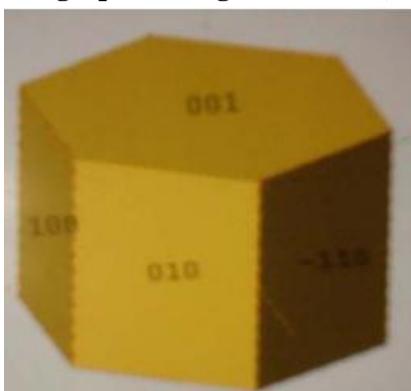**Figure 3: Photograph of the grown $K_3Na(CrO_4)_2$ crystal.**

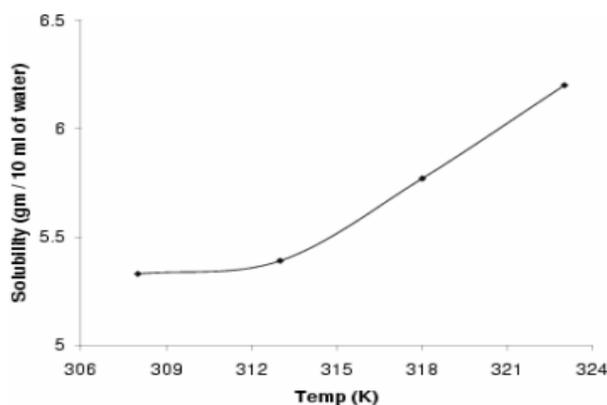**Figure 4: Morphology of $K_3Na(CrO_4)_2$ Crystal.**

Figure 5: Solubility curve of $K_3Na(CrO_4)_2$.

The solubility of the KNCr crystal has been discovered at various temperatures and the solubility curve was drawn which is appeared in the Figure 5.

3. DENSITY ESTIMATION

The density of the crystal was estimated utilizing Archimedes guideline in carbon tetrachloride. The density of the grown sample at room temperature is observed to be 2.76 gm/cm^3. This is near the detailed computed value of 2.77 gm/cm^3 [4.8] and 2.766 gm/cm3. Krajewski et al

announced the deliberate value of density as 2.77 gm/cm^3.

Powder X-Beam Diffraction Of K$_3$na (Cro$_4$)$_2$

The crystals were powdered well and the sample powder is utilized for X– beam examination. The X-beam powder diffraction were taken utilizing X-beam diffractometer, (Bruker, D8 Advance) with Cu KD (λ= 1.542 Å) as source, at a scanning velocity of 2°/min in the 2 T range 5° - 80°.

Figure4.6 demonstrates the XRD example of K$_3$Na (CrO$_4$)$_2$ crystal. The outcomes are in well agreement with the JCPDS document and the *hkl*

planes are distinguished. The announced and recognized *hkl* values are given in the table 1.

The interfacial angles of the crystal are estimated utilizing a contact goniometer. By knowing the cross section parameters, crystal framework and space group one can develop a stereographic plot (Figureure 4.7 and Figureure 4.8) by utilizing the computer program 'Jcrystal'. The normal countenances of the sample have been recognized by the strategy discussed in section 2. The deliberate and Figureured interfacial angles are appeared in table 2.
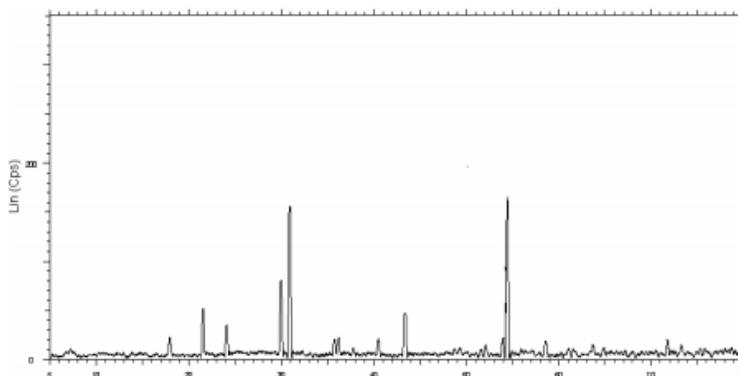

Figure 6: Room temperature XRD pattern of the grown K$_3$Na (CrO$_4$)$_2$ crystal.

Table 1: Comparison of reported and identified *hkl* values of K$_3$Na (CrO$_4$)$_2$ crystal.

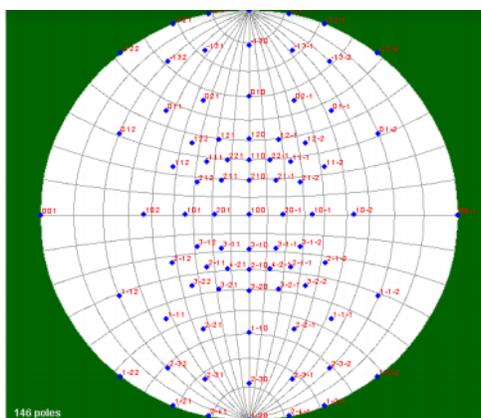| Reported values		Identified	values
d	*hkl*	d	*hkl*
5.0723	100	4.9537	100
4.2053	101	4.1307	101
3.7605	002	3.6979	002
3.0208	102	2.9821	102
2.9285	110	2.8930	110
2.5070	003	2.4797	003
2.2474	103	2.2258	103
2.1026	002	2.0849	002
1.7829	023	1.7693	023
1.7080	212	1.6964	212
1.6907	300	1.6832	300
1.5822	114	1.5738	114
1.4642	220	1.4591	220
1.3380	115	1.3133	115

Figure 7: Stereographic projection of K$_3$Na (CrO$_4$)$_2$crystal projected at 100 direction
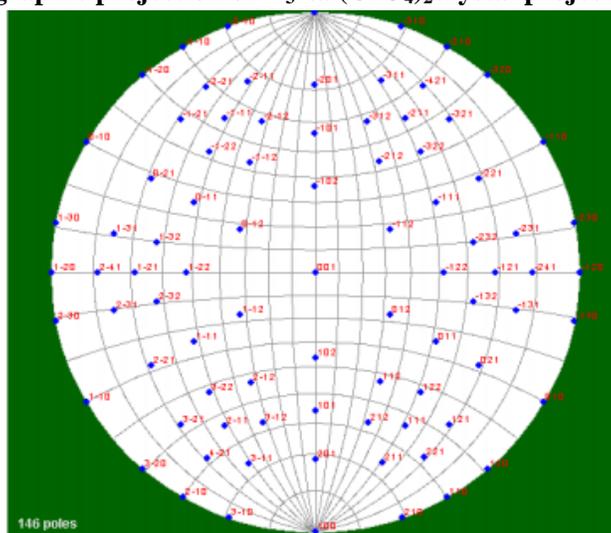

Figure 8: Stereographic projection of K$_3$Na (CrO$_4$)$_2$crystal projected at 001 direction

Table 2: Values of measured and computed interfacial angles of K$_3$Na (CrO$_4$)$_2$ crystal.

Crystal faces		Interfacial angle between faceComputedfrom'Jcrystal'	
Face 1	Face 2	Measuredfrommorphology	
001	010	90.00	89.99
001	100	90.00	89.99
001	-110	90.00	89.99
001	-100	90.00	89.99
010	100	59.871	59.99
010	-110	60.064	59.99
010	-100	120.128	120.00
100	-100	180.00	180.00
-100	-110	60.063	60.00

The samples have been cut utilizing a moderate speed diamond wheel saw as discussed The samples are cleaned utilizing cerium oxide powder to optical refection level.

4. CONDUCTIVITY ANALYSIS

Frequency dependent conductivity spectra

Dependence of ac conductivity on frequency can be communicated by the accompanying equation

$$\sigma total\ (Z) = \sigma\ (0) + A\omega^s$$

This equation is known as Jonscher's Universal Power Law equation where An is the pre exponential factor and s is the frequency example which is for the most part not exactly or equivalent to one. Figure 9 and 10 demonstrate the frequency dependence of estimatedielectrically conductivity for aand c tomahawks at various temperatures.
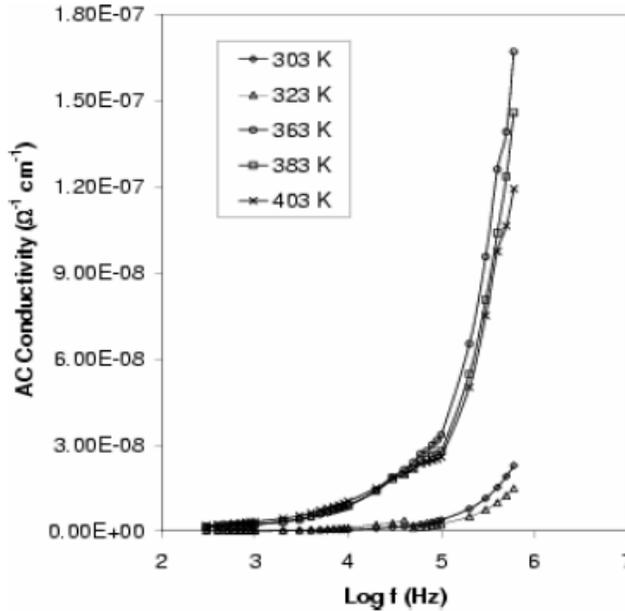

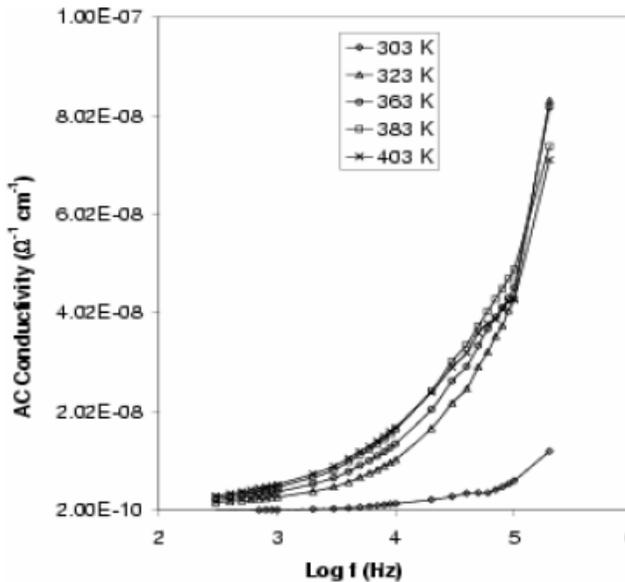**Figure 9: Variation of measured ac conductivity with frequency along a-axis.**

Figure 10: Variation of measured ac conductivity with frequency along c-axis

From the Figures plainly the deliberate ac electrical conductivity is an expanding capacity of frequency for the two tomahawks. At lower frequencies and higher temperatures, the deliberate ac conductivity is somewhat higher than dc conductivity and the commitment because of unadulterated ac conductivity is distinguishable. At higher frequencies and higher temperatures, the commitment of unadulterated ac conductivity to the aggregate conductivity is all the more, however the commitment of dc conductivity can't be disregarded. At higher frequencies and lower temperatures, unadulterated ac conductivity commitment to add up to ac conductivity totally prevails over that because of dc conductivity.

At lower frequencies the likelihood of between well hopping prevails over that due to intra-well hopping and aggregate conductivity around equivalent to the dc conductivity. As the flag frequency is expanded to higher values, the likelihood of event of intra-well hopping does increment and unadulterated ac conductivity contribute much to add up to conductivity.

The value of' s' in the above equation is the incline of the plot of $\ln\sigma_{ac}$ against $\ln$ ($\omega = 2\,\pi f$). The dc conductivity can be extricated from the aggregate conductivity and pre exponential factor An is the slant of the plot of σ_{total} against ω^s. The ac conductivity can be theoretically Figure utilizing the above values, by the power law parameters in the Universal Power Law equation. The theoretically fitted bend is nearly same as that of the exploratory values. The assessed control law parameters are given in the tables 3 and 4.

Table 3: Power law Parameters of $K_3Na\,(CrO_4)_2$ for different temperatures along a-axis.

Temperature (K)	V(0) $(\Omega^{-1}cm^{-1})$	s	A
303	2.75 u 10^{-11}	0.76946	1.2494 u 10^{-13}
323	1.56 u 10^{-12}	0.5802	1.1291 u 10^{-12}
363	4.4 u 10^{-10}	0.6425	6.5862 u 10^{-12}
383	7.0 u 10^{-10}	0.6096	4.2599 u 10^{-11}
403	1.0 u10^{-9}	0.5543	1.6975 u10^{-11}

Table 4: Power law Parameters of $K_3Na\,(CrO_4)_2$ for different temperatures along c-axis.

Temperature (K)	V(0) $(\Omega^{-1}cm^{-1})$	s	A
303	1.5 u 10^{-11}	0.7239	5.5454 u 10^{-13}
323	9.0 u 10^{-10}	0.6853	4.5931 u 10^{-12}
363	1.0 u 10^{-9}	0.6227	1.134 u 10^{-11}
383	1.5 u 10^{-9}	0.6245	1.1927 u 10^{-11}
403	1.6 u10^{-9}	0.5670	2.2875 u10^{-11}

Plainly σ (0), s and a are temperature dependent amounts. The value s ranges in the vicinity of 0.77 and 0.55 for an axis and in the vicinity of 0.72 and 0.57 for c-axis. Theoretical fitting was finished utilizing the above equation for all temperatures. A decent agreement amongst exploratory and theoretical fitting was watched.

5. CONCLUSION

The conductivity and dielectric investigations of $K_3Na(CrO_4)_2$ single precious stone demonstrates a recently watched conceivable stage transition in the gem at around 326 K. DSC think about additionally underpins this perception. More examination had to know the idea of this stage transition. From the perplexing impedance examination the ionic idea of conductivity is uncovered. The variation of conductivity with frequency shows that at lower frequencies between well hopping prevails over that due to intra-well hopping and at high frequencies the likelihood of event of intra-well hopping increases.

REFERENCES

[1].   P. B. Moore, Complex crystal structures related to glaserite $K_3Na(So_4)_2$, evidence for very dense packing among oxylates, *Bulletin de la societeFrancaise de Mineralogieet de Cristsllographie*,**104**, 536-547, (2011).

[2].   Mathai Mathew and Shozo Takagi, Structures of Biological Minerals in Dental Research, *Journal of Research of the National Institute ofStandards and Technology,* Vol.**106**, Pages 1035-1044, (2001).

[3].   Ph.DThesies, NachiappanArumugam, New Ternary Alkali Oxides and Quaternary Alkali Oxy-Nitrides of Molybdenum and Tungsten, *Max-Plank-Institut fur Festkorperforschung*, Stuttgart University, Stuttgart,(2005).

[4].   V.A.Morozov,   B.I.Lazoryak,   A.P.Malakho,K.V.Pokholok, S.N.PolyakovandT.P.Terekhina, The Glaserite- like Structures of Double Sodium and Iron Phosphate $Na_3Fe(PO_4)_2$, *Journal of Solid State Chemistry***160**, 377-381, (2001).

[5].   AllaArakcheeva, GervaISChapuis, Vaclav Petricek, Michal Dusek and Andreas Schonleber, *The incommensurate Structure of $K_3ln(PO_4)_2$,*ActaCryst, **B59**,17-27, (2003).

[6].   H.S.Washington and H.E.Merwin, Aphthitalite from Kilauea, *AmericanMineralogist,* Vol.**6**, Pages 121-125, (2011).

[7].   F.Khlissa, A.M`nif, R.Solimando and R.Rokbani, Prediction of mineral precipitation during isotherm evaporation of southern Tunisian natural brines, *Desalination***166***,* 261-266, (2004).

[8].   B. Gossner, *Neues. Jahrb. F. Mineral,***57A***,* 89-116, (2008).

[9].   A. Bellanaca, Sulla Struttura dell` aftitalite, period, *Di Mineral,***14**, 67-97, (2003).

[10].   Pontonnier, L.M.Caillet and S. Aleonard, *Mat. Res. Bull,***7**, 799-812, (2012).

[11].   P. B. Moore., *Am. Mineral,***58**, 32-42, (2003)